Environ Earth Sci (2015) 73:7669–7677
DOI 10.1007/s12665-014-3941-y

CrossMark

ORIGINAL ARTICLE

Mechanochemical treatment and structural properties of lead adsorption on kaolinite (Rudovci, Serbia)

Snežana S. Nenadović · Ljiljana M. Kljajević · Miloš T. Nenadović · Miljana M. Mirković · Smilja B. Marković · Zlatko Lj. Rakočević

Received: 17 October 2014 / Accepted: 4 December 2014 / Published online: 19 December 2014

Abstract In the present work, remediation of lead-containing solution using raw and modified kaolinite has been presented. The micro and nanostructure of samples has been characterized by X-ray diffraction (XRD), scanning electron microscopy (SEM) and atomic force microscopy (AFM). Laser diffraction and scattering (LDS), was analyzed by particle size analyzer based on laser diffraction and particle size distribution (PSD) was done. The degree of metal adsorption was evaluated analyzing the Pb(II) contaminated samples by inductively coupled plasma atomic emission spectrometry (micro- and nanostructure on immobilization efficiency correlCP AES). The results show the impact of immobilization efficiency and ation between micro- and nanostructure. The thermodynamic data ($\Delta H°$, $\Delta S°$, $\Delta G°$) are calculated from the temperature-dependent sorption isotherms. The results suggest sorption process of Pb(II) on kaolinite as spontaneous and endothermic.

Keywords Kaolinite · Micro–nanostructure · AFM phase analysis · SEM · Particle size distribution

S. S. Nenadović (✉) · L. M. Kljajević · M. M. Mirković
Laboratory for Materials Sciences, Institute of Nuclear Sciences Vinča, University of Belgrade, P.O. Box 522, 11000 Belgrade, Serbia
e-mail: msneza@vinca.rs

M. T. Nenadović · Z. Lj. Rakočević
Laboratory for Atomic Physics, Institute of Nuclear Sciences Vinča, University of Belgrade, P.O. Box 522, 11000 Belgrade, Serbia

S. B. Marković
Institute of Technical Sciences of the Serbian Academy of Sciences and Arts, University of Belgrade, Knez Mihailova 35/IV, 11000 Belgrade, Serbia

Introduction

In the twenty-first century, environmental pollution is one of the major threats to human life. Among the different types of pollution, waste water stream which contains heavy metals is one of the major problems due to a large amount of water used in our daily life. There are numerous sources of industrial effluents leading to heavy metal discharges apart from the mining and metal-related industries. Because of their toxicity and non-biodegradable nature, heavy metals are of special significance. One of contaminating heavy metals is lead which is widespread in urban and industrial areas as a consequence of different industrial activities and by-products, gasoline processing as well as production of painting materials and their use (Mart'inez and Motto 2000; Paff and Bosilovich 1995). Inhalation and ingestion of lead may cause various health diseases (Needleman and Bellinger 1991). In addition, lead in soils may adversely affect soil ecology, agricultural production, or product and water quality (Wang et al. 2001). Among all that has been mentioned, for the elimination of lead from the environment it is important to find a suitable medium for its adsorption. The use of alternative low-cost natural materials, as potential sorbents for the removal of heavy metals has been stressed nowadays. These cost-effective materials range from industrial by-products or waste, to agricultural products and other known natural materials like clay, zeolites, diatomite (Montinaro et al. 2007; Sheng et al. 2008; Sljivic et al. 2008).

Kaolinite is one of the well-known low-cost natural clay, available worldwide in rocks as crystalline structure. The kaolinite structure possesses great advantages in many processes due to its high chemical stability and low expansion coefficient. It is a 1:1 aluminosilicate consisting of chemical composition SiO_2, 42.14 mol%; Al_2O_3,

15.61 mol% and H_2O, 42.25 mol% (James 1995) and crystalline structure consists of stacked pairs of tetrahedral silica sheets and octahedral alumina sheets. The surfaces of kaolinite are believed to carry a constant structural negative charge due to the isomorphous substitution of Si^{4+} by Al^{3+} in silica layer, whereas the charge on the alumina face and on the edges due to the protonation/deprotonation of exposed hydroxyl groups depend on the pH of the solution (White 1987). The heavy metal adsorption capability of kaolinite is not so high due to its lower cation exchange capacity. Its Cu^{2+}, Ni^{2+} and Fe^{3+} adsorption capacities are 0.67, 10.4, and 11.2 mg/g, respectively (Bhattacharyya and Gupta 2008; Wang et al. 2009). Li et al. (2011) developed a novel environment-friendly kaolinite composite, which has an exceptional Cu^{2+} adsorption capability and can be easily removed from aqueous solution. To best knowledge of effect mechanochemical activation started to be considered (Montinaro et al. 2007) as a possible method for improvement of sorption properties of natural materials as well as clay and diatomite. Mechanochemical activation involves simple grinding of an inorganic material and this would lead to physical disintegration along with the formation of active surfaces as well as changes in the physicochemical behavior of materials. Generally this kind of process as applied to crystalline solid produces a loss of crystallinity (amorphinization) (Boldgrev and Avvakumov 1971) together with the increase in surface energy and surface reactivity of the material and consequently in chemical activity (Butyagin 1971). Changes in the mechanical and chemical properties of the clay are discussed as the interactions of the heavy metal cations with the kaolinite which affect the structure of the kaolinite and influence properties such as swelling capacity, compaction capability and the double-layer behavior. Using the adsorption data, the reactions at the clay–water interphase and the probable effects on the physical properties and structure of kaolinite are discussed in the study of Miranda-Trevino and Coles (2003). They studied the adsorption behavior of kaolinite at three different concentrations of Pb, Zn and Cd during different periods of exposure. The kaolinite retained up to 10.0 μmol/g of Pb and in any case, the adsorption reduced the solution pH from 4.6 to 3.7. Suraj et al. (1997) used two methods of micronization (ball milling and oscillatory milling) for the purpose of investigating the effect of micronization on the crystalline structure of kaolinite clay mineral and the role of this mechanically modified kaolinite structure on the adsorption ion-exchange properties of toxic heavy metals. Also, mechanically induced reactions have been successfully used for the degradation of organic pollutants such as hexachlorobenzene (Oonnittan et al. 2009), hexabromobenzene (Mulas et al. 1997) and more recently for the degradation of sulfonic acids (Pham et al. 2009).

In this work, kaolinite was analyzed as a potential sorbent for the removal of Pb(II) ions. Furthermore, the effect of surface modification of kaolinite by ball milling on Pb(II) adsorption and on filtration quality was used to improve the sorption properties of natural kaolinite. In order to provide a better explanation of lead adsorption process, detailed examination of the micro-nano structure of raw and modified kaolinite was done by different physicochemical methods.

Experimental part

Materials and methods

The kaolinite used is of high-quality paper-coating grade clay obtained from Rudovci, Lazarevac, Serbia. The sample was used directly without further preparation. Kaolinite from Rudovci (Serbia) was processed by ball milling in a Turbula Type T2C Mixer. The milling was performed under argon using ball-to-powder ratio (BRP) 4.

Turbula Type T2C Mixer mill operating at the standard milling frequency of 870 rpm, was employed together with a stainless steel vial, 606.75 g in weight, having the internal diameter equal to 3.8 cm and the internal height of 5.8 cm. Different kaolinite amounts were introduced inside the vial together with two stainless steel balls of 8 g and 10 mm in diameter in order to investigate the effect of the ball-to-power ratio (BRP). In particular, BRP values of 4, corresponding to kaolinite weights of 25 g was used.

The elemental composition analysis of natural raw kaolinite was conducted by XRF (type UPA XRF 200) and modified forms a expressed as weight percentages of metal oxides.

Chemical analysis of Pb-contaminated samples was performed by means of ICP AES atomic emission spectrometry with inductively coupled plasma (model Spectro CIROS vision, Kleve, Germany).

ICP measurements were performed with the SPECTRO CIROSCCD ICP optical emission spectrometer with radial plasma viewing. The spectrometer in Paschen–Runge mounting consists of a double-grating optical system with 22 CCD detectors. The spectral range between 125 and 770 nm is covered, allowing complete scans of the spectrum within 3 s.

The mineral phase compositions of the materials were characterized by X-ray powder diffraction technique (Al-Ghouti et al. 2005; Goren et al. 2002). The crystal structure of kaolinite before and after mechanical milling was examined by X-ray diffractometer Siemens D-500, with Cu–K_α radiation. The diffracted X-rays were collected over 2θ range 20°–80° using a step width of 0.02° and measuring for 1 s per step.

The morphology and microstructure of the materials were studied by using scanning electron microscopy (SEM) technique. SEM micrographs were performed in a JEOL JSM 6460LV and Oxford Instrument INCA-X-sight at 25 kV scanning electron microscope. The materials were introduced onto a conductive carbon tape and coated with gold to prevent charging. The powdered samples were dispersed in ethyl alcohol and then left to settle on a disc. After drying, each is coated with thin film of carbon using a vacuum evaporator of the electric charges of the incident electron beam on the sample surface.

The surface morphology of the kaolinite was quantified using an atomic force microscopy-AFM. The AFM studies were carried out on Veeco MultiMode Quadrex IIIe in the tapping mode. Cantilever type is standard RTESP-Veeco production. Tip material is 0.5–2 Ω cm phosphorus (n) doped Si. AFM imaging was performed in tapping mode with a 15 to 20 µm-high pyramidal tip. The resonance frequency of tip was 268.2 kHz. The scan rate was maintained in order of 2 Hz to get the optimal image quality.

The particle size distribution was determined by the particle size analyzer (PSA). For the particle size measurements the powder was dispersed in water, in an ultrasonic bath (frequency of 40 kHz and power of 50 W), for 5 min.

Adsorption solutions

Kaolinite samples were contaminated at 25 °C with a solution of $Pb(NO_3)$ (99.99 % Alfa Aesar) concentration 2.95 mg/l. Each sample was dissolved in 10 ml of these solutions in the flasks. The flasks were sealed and shaken for 24 h, which was experimentally proved to be a sufficient time to reach equilibrium conditions. Finally, the solutions were sampled in order to determinate the solute concentrations. The concentrations of Pb(II) in the kaolinite phase at equilibrium were determined using ICP method. Concentrations were calculated through the following mass balance:

$$q^{24h}_{Pb(II)} = \frac{(C^{\circ}_{Pb(II)} - C^{24h}_{Pb(II)})}{W_{solid}} \times V_{liq}, \quad (1)$$

where $q^{24h}_{Pb(II)}$ (mg kg^{-1}) is the Pb(II) concentration in the kaolinite phase after 24 h of contact, $C^{\circ}_{Pb(II)}$ and $C^{24h}_{Pb(II)}$ (mg l^{-1}) are the initial and equilibrium concentration of Pb(II) in the liquid phase, respectively, V_{liq} (l) in the volume of liquid solution and W_{solid} (kg) is the kaolinite weight contacted with the lead ions. Immobilization efficiency, after each treatment interval, was calculated using following equation:

$$\eta(t)\% = \left(1 - \frac{C_{Pb(II)}(t) \cdot V_{leach}}{q^{24h}_{Pb(II)} \cdot W_{solid}}\right) \times 100, \quad (2)$$

where $\eta(t)$ % is the immobilization efficiency (%) of the milling treatment for a time interval equal to t (s), C_{Pb} (mg l^{-1}) is the Pb(II) concentration in the sample, V_{leach} is leachate volume (Eq. 2), $q^{24h}_{Pb(II)}$ (mg kg^{-1}) is the initial Pb(II) concentration in the untreated kaolinite (Eq. 1) and W_{solid} (kg) is the kaolinite weight undergone which was measured in the test.

The distribution coefficient, K_d is calculated from the following equation:

$$K_d = \frac{\left(C^{\circ}_{Pb(II)} - C^{24h}_{Pb(II)}\right)}{C^{24h}_{Pb(II)}} \times \frac{V_{liq}}{W_{solid}}. \quad (3)$$

Thermodynamic study

The thermodynamic (ΔH°, ΔS° and ΔG°) for Pb(II) sorption onto kaolinite can be determined from the temperature dependence. Free energy changes (ΔG°) are calculated from the relation:

$$\Delta G^{\circ} = -RT \ln K^{\circ} \quad (4)$$

where R is the universal gas constant (8.314 J/mol K), T is the temperature in Kelvin and K° is the sorption equilibrium constant. Values of ln K° are obtained by plotting $\ln K_d$ vs. C_{eq} to zero, the value of the intercept is the value of ln K° (Montinaro et al. 2007, 2008).

Standard entropy changes are calculated using the equation:

$$\left(\frac{\partial \Delta G^{\circ}}{\partial T}\right)_P = -\Delta S^{\circ}. \quad (5)$$

The average standard enthalpy change (ΔH°) is then calculated from the relationship:

$$\Delta H^{\circ} = \Delta G^{\circ} + T\Delta S^{\circ}. \quad (6)$$

Results and discussion

Micro–nanostructure properties of kaolinite

The main chemical composition of the kaolinite is given in Table 1. The main components of the natural raw kaolinite are oxides of Si, Al and Fe (SiO_2, Al_2O_3, Fe_2O_3). There are

Table 1 Chemical composition of the kaolinite

	SiO_2	Al_2O_3	Fe_2O_3	TiO_2	$CaCO_3$	MgO	LoI*
Chem. comp. (wt%)	55.50	24.6	10.13	0.12	0.67	0.34	8.64

* Lost on ignition

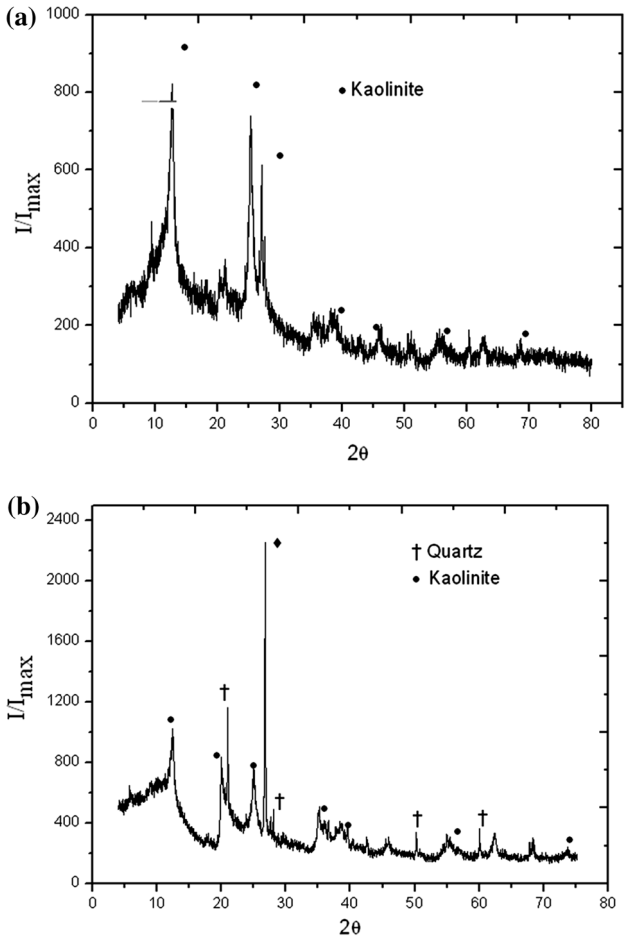

Fig. 1 XRD analysis of **a** raw kaolinite and **b** 5-h milled kaolinite

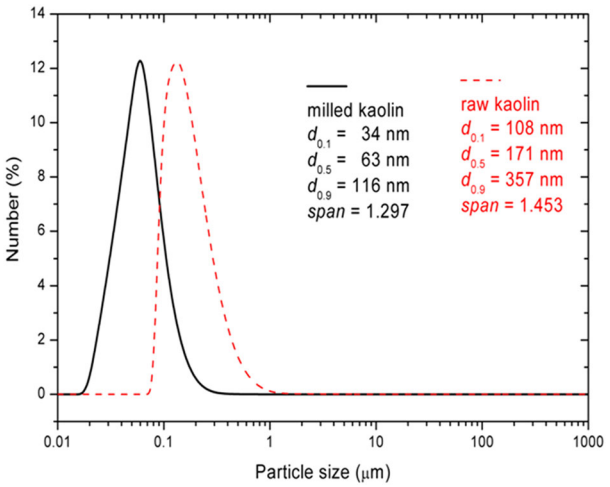

Fig. 2 Particle size distribution for raw kaolinite and 5-h milled kaolinite

also water molecules (not mentioned in table) and impurities consisting of $CaCO_3$, Fe_2O_3, TiO_2.

The XRD patterns of the as received (Fig. 1a), and of the mechanically treated samples (Fig. 1b) depict the following mineral phases: kaolinite, illite, quartz.

The use of high-energy ball milling to induce structural defects amorphization, microstructural refinement, vacancies and dislocations resulting in a loss of crystallinity of soil compounds is a well-documented method (Suryanarayana 2001).

No clay minerals were found in the Rudovci kaolinite even in trace amounts as there is no any XRD peak that could be characteristic for new phases, contrary to many soils samples from other origins.

The semiquantitative mineralogical composition was determined based on relative peak intensities (mostly of lower orders) and peak areas corrected by various factors (Riedmüller 1978). Despite the fact that the Hinckley crystallinity index is not widely used because it is influenced by the presence of quartz, feldspar, iron oxides and other clay minerals, it remains an empirical estimate of the kaolinite degree of crystallinity.

Results of the particle size distribution, based on number, of the analyzed kaolinite samples are presented in Fig. 2. Here, we emphasized that the correctness of the measurement depends on the degree of the powder dispersion. So, after 5 min of powder dispersion in water with the aid of low-intensity ultrasound, the following results were obtained: in *K* type (raw kaolinite) the particle size distribution was relatively narrow (span = 1.453) where 10 % of particles ($d_{0.1}$) have diameter smaller than 108 nm, 50 % of particles ($d_{0.5}$) possess diameter of 171 nm, while 90 % of particles ($d_{0.9}$) are smaller than 357 nm. After 5 h of milling, the particle size distribution become narrower (span = 1.297) and particles' dimension where reduced, $d_{0.1}$ was 34 nm, $d_{0.5}$ 63 nm, and $d_{0.9}$ is 116 nm. From these results it can be concluded that milling of kaolinite yield particles reduction up to 3 times on average.

SEM and AFM show the surface morphology of kaolinite before and after milling (Figs. 3, 4). The resulting sample is characterized by flaky shape with a typically layered card house structure of kaolinite. The shape of raw kaolinite seems to be formed by dense sheets where regular kaolinite particles ranges in all sizes. There is some kind of ordering where smaller particles surround the larger ones. However, the flaky structure of raw kaolinite was changed into fractional and grain structure resulted in the modification due to mechanochemical activation. After the modification, the layers of raw kaolinite were broken, leading to more micro-sized particles and higher specific surface.

In Fig. 4 AFM micrographs of the kaolinite are presented. Pictures sizes in both cases are 2 × 2 μm. Figure 4a presents topography of the kaolinite. Small kaolinite particles are compacted under the force into the pellet. It is obvious that the hexagonal shape is present. This is a proof of a close

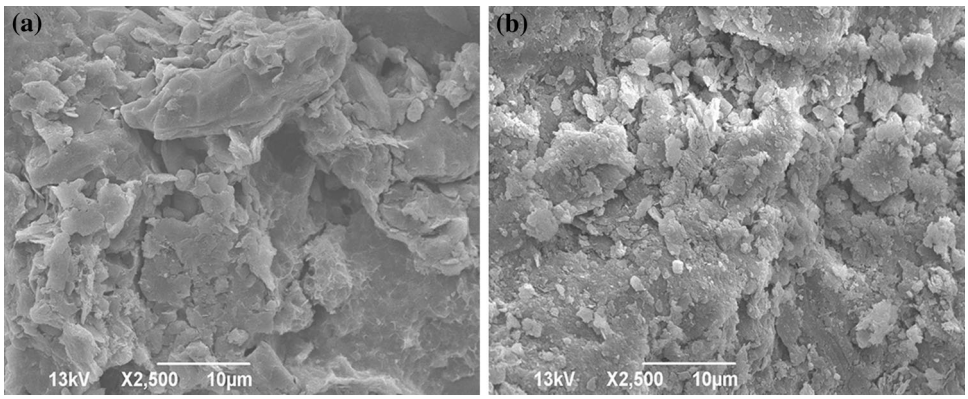

Fig. 3 SEM of **a** raw kaolinite and **b** 5-h milled kaolinite

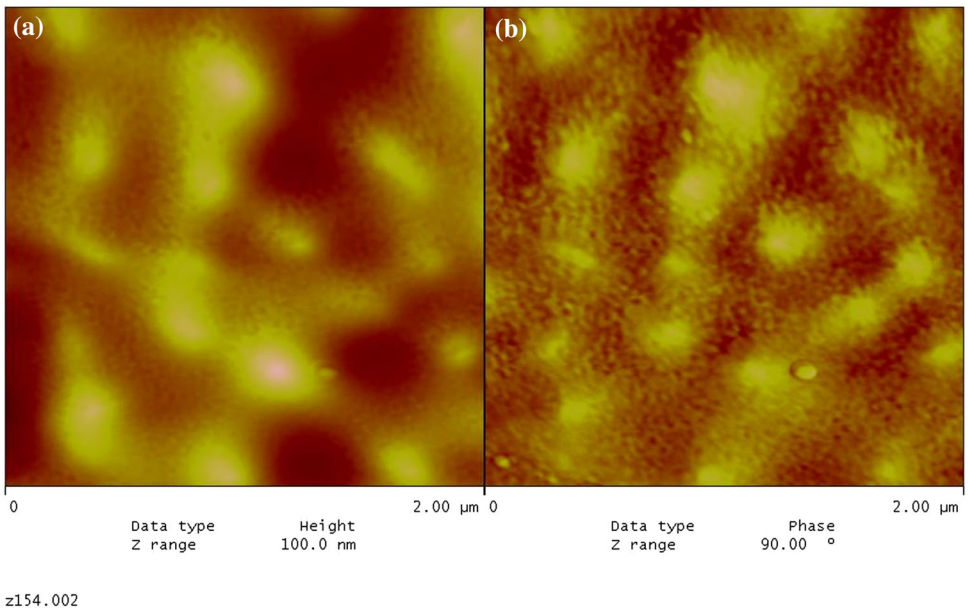

Fig. 4 AFM image (2 × 2 µm) of raw kaolinite: **a** topography, **b** phase structure

package in the lattice of kaolinite. Unit cells are very close and they make a sponge-like structure with the pore sizes close to Pb ion size which allow entering in kaolinite. Figure 4b presents phase composition of the kaolinite. Like a natural material, kaolinite is very pure. One can notice that there are only two phases of this material, which are Si and Al. AFM phase analysis in Fig. 4b very clearly shows differentiation of sample phase composition. Light and dark fields are present on this image. We can suggest that light field can be Si phase. Dark field can be mainly composed from Al and Fe phase. This is in a good agreement with a chemical composition of kaolinite (Table 1). In kaolinite there is one Al-octahedral sheet which is bonded to one Si-tetrahedral sheet by shared (apical) oxygen atoms of the tetrahedral sheet. Two adjacent layers are held together by hydrogen bonding. Consequently, the structure is fixed and no expansion occurs between layers when the clay is wetted. The effective surface of kaolinite is restricted to its external surface area. The typical kaolinite particle is fairly large (thickness ~50 nm and width ~1–3 nm) in comparison with other clay particles and hexagonal in shape. Because of the strong binding forces between their structural layers, kaolinite particles are not readily broken down into extremely thin plates. Kaolinite exhibits very little shrinkage and swelling (James 1995).

From the higher magnification (1 × 1 µm) of the same sample we obtained a more clear explanation on the atomic level (Fig. 5). The hexagonal structure of kaolinite unit cell is clearly visible. The average diameter of single hexagon is 50 nm. These unit cells are close, making a terrace structure of each hexagon. Hexagon unit cells can be multilayered, which is not clearly visible with AFM analysis, because this technique deals with the surface topography. In this layered structure basic Si and Al atoms can be randomly distributed.

Figure 6 represents the ball milled kaolinite samples for 5 h. During the milling process, topography of this sample had undergone a change. The sponge-like structure is more

prominent. Hexagonal unit cells are no more clearly visible. Kaolinite has become more dense and compact (Fig. 6a). During the ball milling process the unit cell has been partially destroyed and effective diameter of pore is decreased. Phase structure has also been changed. Ratio of the light and dark fields (Fig. 6b) is different from the one in the untreated sample. This can suggest that the real chemical composition is changed during milling. It can be a proof of a better sorption ability of 5 h milled kaolinite.

In Fig. 7 the 3D surface topography is presented. Magnification of this figure is 1 × 1 μm. Comparing Fig. 7 with Fig. 4 one can notice the structural and topography changes caused by milling. Hexagonal unit cells have disappeared and instead of them, agglomerates with a sponge-like structure appear. The basic unit cell structure is destroyed. Some indication of hexagonal shape is preserved, but only a few percentage of a basic structure remain preserved. Similar results are obtained using SEM analysis (Fig. 3). AFM phase diagrams analysis of raw and 5 h of milled kaolinite is shown in Fig. 8. Significant differences in the composition are clearly visible. Peak displacement values along the *x*-axis represent the relative chemical changes on the surface of kaolinite. Phase composition of pure kaolinite has almost Gaussian distribution and a single peak at 33.55°. Milled kaolinite shows expansion of the total phase composition, the base peak shift from 33.55° to 26.00° and the emergence of a new peak at 42.50°. These changes can be attributed to mechanochemical reactions that result from milling process. They can contribute to better adsorption characteristics of 5-h milled kaolinite.

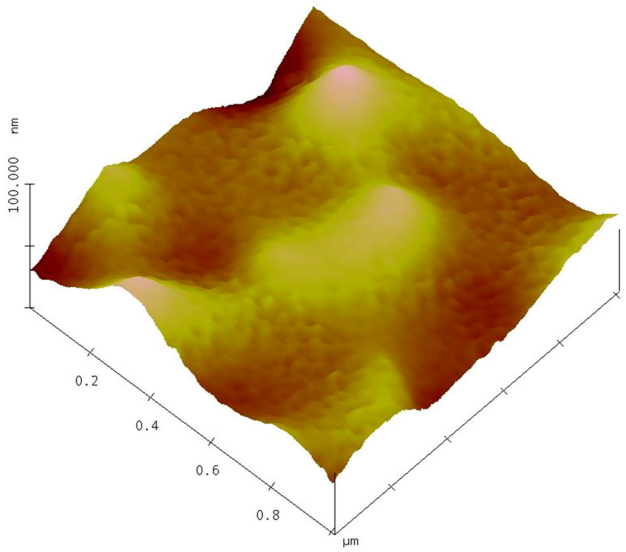

Fig. 5 AFM 3D surface topography of raw kaolinite (1 × 1 μm)

Immobilization efficiency and adsorption potential of Pb ions

Raw kaolinite and five milled samples from 1 to 5 h have been investigated as potential material for remediation of wastewater specially Pb(II). According to Montinaro et al. (2008), for BPR (ball-to-powder ratio) 4, the best diatomite immobilization efficiency (up to 97 %) has been achieved and this BPR as standard value in our experiment is established (Nenadovic et al. 2009).

In Fig. 9, Pb(II) concentration in the kaolinite phase after 24 h and immobilization efficiencies of kaolinite samples versus milling time are presented. One can notice that quantity of absorbed Pb(II) increase with milling time and

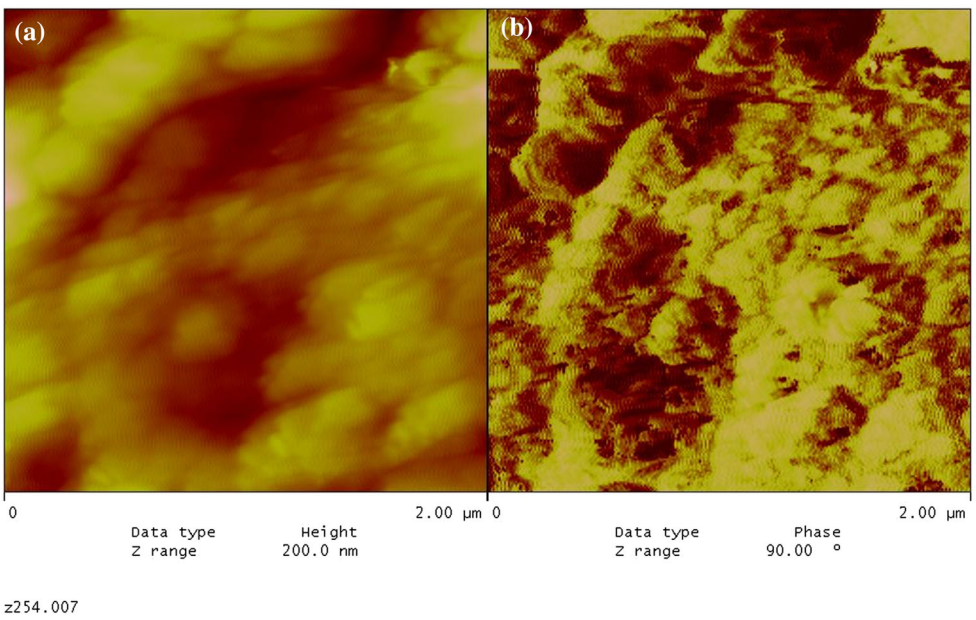

Fig. 6 AFM image (2 × 2 μm) of 5-h ball milled kaolinite samples: **a** topography, **b** phase structure

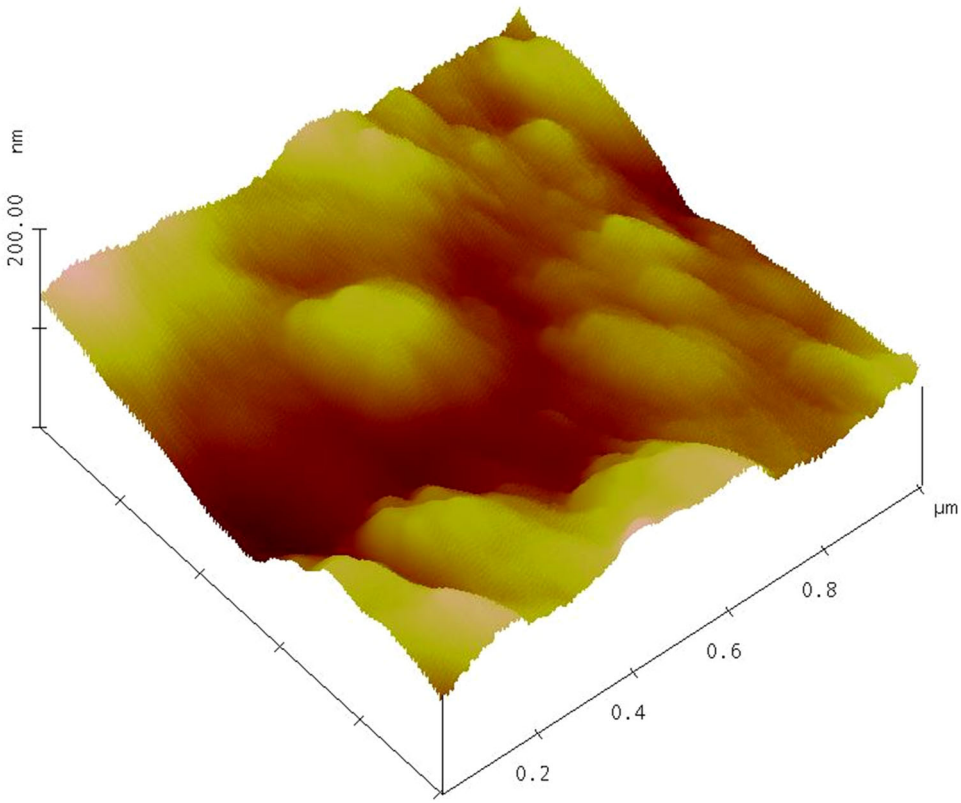

Fig. 7 AFM 3D surface topography (1 × 1 µm) of the 5-h ball milled kaolinite sample

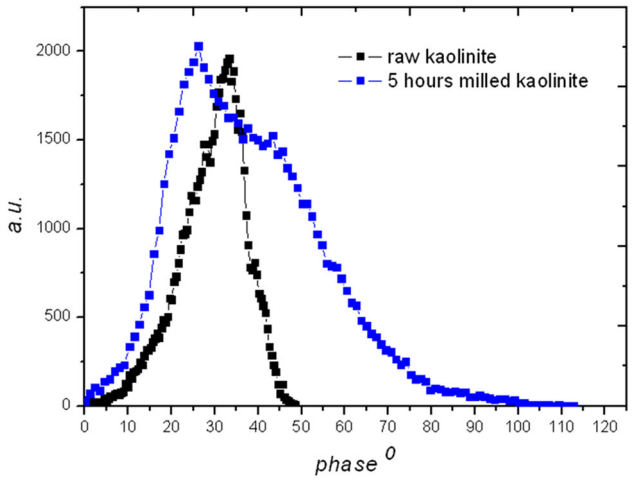

Fig. 8 AFM phase composition histogram of raw and 5-h milled kaolinite

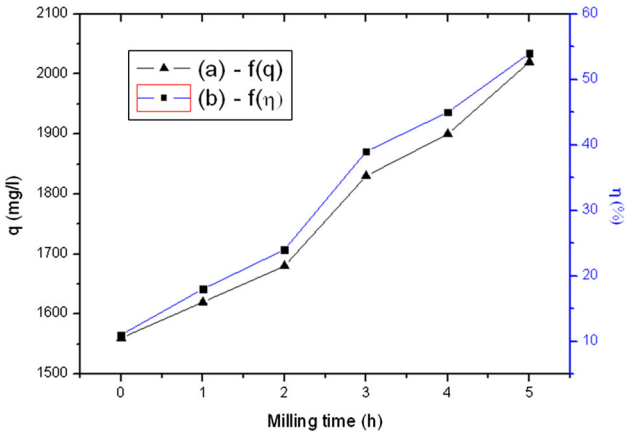

Fig. 9 Pb(II) concentration in the kaolinite phase after 24 h (**a**); immobilazation efficiences of kaolinite samples (**b**)

achieves the saturation when milling time is 5 h. This can be ascribed taking into account microstructural changes that emerged after ball milling such as appearance of mesoporous sponge-like structure. Similar results were obtained taking into account immobilization efficiency. The maximum efficiency of 54 % is obtained after 5 h of ball milling.

On the basis of Eq. (3), from linear fit of $\ln K_d = f(C^{24h}_{Pb(II)})$ Sheng et al. (2008) has obtained value of $\ln K^\circ$ (see Fig. 10) and other thermodynamic parameters (ΔG° and ΔS°) for Pb(II) sorption onto kaolinite. These parameters of Pb(II) sorption are presented in Table 2.

The evaluation of thermodynamic parameters provides an insight into the mechanism of Pb(II) sorption on kaolinite. The free energy of Pb(II) sorption on kaolinite is more negative at 298.15 K, which suggests that the spontaneity of the process increases with the rise in temperature. A positive value of the standard enthalpy change

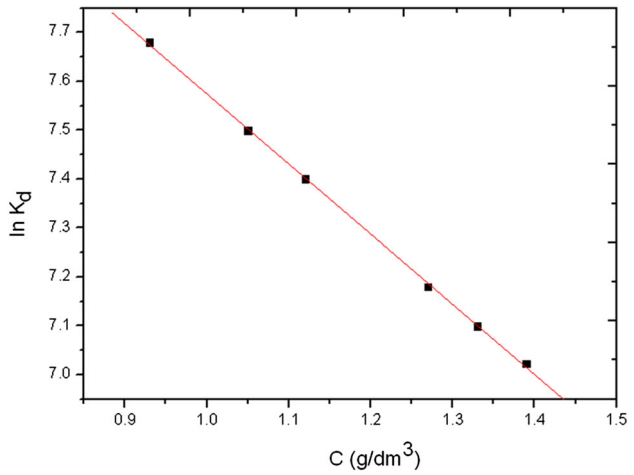

Fig. 10 Linear fit of ln $K_d = f(C^{24h}{}_{Pb(II)})$

Table 2 Thermodynamic parameters of Pb(II) sorption on kaolinite

T (K)	ΔG° (kJ/mol)	ΔS° (J/molK)
298.15	−22.329	74.98

($\Delta H°$) indicates that the sorption is endothermic. The low value of $\Delta H°$ also suggests that the endothermic process of Pb(II) sorption on kaolinite is weak. This conclusion is supported by the weakly increasing sorption with the increase in temperature. Since the free energy changes are negative and accompanied by positive entropy changes, the sorption reactions are spontaneous with a high affinity.

Conclusion

The adsorption phenomena of Pb(II) ions onto kaolinite from Rudovci location (Serbia) were investigated. Mechanochemical treatment reveals that adsorption of heavy metals (Pb) on kaolinite increase its absorption behavior which is confirmed by possibility of adsorption not only on the basis of chemical analysis and ICP, but this result is confirmed by AFM analysis when compared not only with grounded sample but with the sample after 5-h milling. X-ray showed that the particle size decreased and that this affects the adsorption of Pb(II) ions. Results of the particle size distribution of the distribution of the analyzed kaolinite have shown that milling yields particles up to 3 times on average. All this can contribute to the fact that 5-h milled kaolinite has shown a better adsorption capacity. Reduction of the main particle size and changes in the ordered crystalline structure of the raw kaolinite, done by mechanical milling, have improved its adsorption potential of Pb(II) ions. In the future, the potential of other heavy metals should be examined and compared with the results obtained for Pb(II).

Acknowledgments This project was financially supported by the Serbian Ministry of Education and Science on projects 45005 and 45012.

References

Al-Ghouti M, Khraisheh MA, Ahmad MN, Allen S (2005) Thermodynamic behaviour and the effect of temperature on the removal of dyes from aqueous solution using modified diatomite: a kinetic study. J Colloid Interface Sci 287(1):6–13

Bhattacharyya KG, Gupta SS (2008) Kaolinite and montmorillonite as adsorbents for Fe(III), Co(II) and Ni(II) in aqueous medium. Appl Clay Sci 40:1–9

Boldgrev VV, Avvakumov EG (1971) Mechanochemistry of inorganic solids. Russ Chem Rev 40:847–859

Butyagin PY (1971) Kinetics and nature of mechanochemical reactions. Russ Chem Rev 40:905–915

Goren R, Baykara T, Marsoglu M (2002) A study on the purification of diatomite in hydrochloric acid. Scand J Metall 31(2):115–119

James SR (1995) Principles of ceramics processing, 2nd edn. Wiley, New York

Li Y, Xia B, Zhao Q, Liu F, Zhang P, Du Q, Wang D, Li D, Wang Z, Xia Y (2011) Removal of copper ions from aqueous solution by calcium alginate immobilized kaolin. J Environ Sci 23(3):404–411

Mart'ınez CE, Motto HL (2000) Solubility of lead, zinc and copper added to mineral soils. Environ Pollut 107:153–158

Miranda-Trevino JC, Coles CA (2003) Kaolinite properties, structure and influence of metal retention on pH. Appl Clay Sci 23(1):133–139

Montinaro S, Concas A, Pisu M, Cao G (2007) Remediation of heavy metals contaminated soils by ball milling. Chemosphere 67(4):631–639

Montinaro S, Concas A, Pisu M, Cao G (2008) Immobilization of heavy metals in contaminated soils through ball milling with and without additives. Chem Eng J 142:271–284

Mulas G, Loiselle S, Schiffini L, Cocco G (1997) The mechanochemical self-propagating reactions between hexachlorobenzene and calcium hydride. J Solid State Chem 129:263–270

Needleman HL, Bellinger DD (1991) The health effects of low level exposure to lead. Annu Rev Public Health 12:111–140

Nenadovic S, Nenadovic M, Kovacevic R, Matovic Lj, Matovic B, Jovanovic Z, Grbovic-Novakovic J (2009) Influence of diatomite microstructure on its adsorption capacity for Pb(II). Sci Sinter 41(3):309–317

Oonnittan A, Shrestha RA, Sillanpää M (2009) Removal of hexachlorobenzene from soil by electrokinetically enhanced chemical oxidation. J Hazard Mater 162:989–993

Paff SW, Bosilovich BE (1995) Use of lead reclamation in secondary lead smelters for the remediation of lead contaminated sites. J Hazard Mater 40:139–164

Pham TD, Shrestha RA, Sillanpää M (2009) Electrokinetic and ultrasonic treatment of kaoline contaminated by POPs. Sep Purif Technol 44:2410–2420

Riedmüller G (1978) Neoformation and transformation of clay minerals in tectonic shear zones. Minerol Petrol 25:219–242

Sheng G, Hu J, Wang X (2008) Sorption properties of Th(IV) on the raw diatomite—effects of contact time, pH, ionic strength and temperature. Appl Radiat Isot 66(10):1313–1320

Sljivic M, Smiciklas I, Pejanović S, Plecas I (2008) Comparative study of Cu^{2+} adsorption on a zeolite, a clay and a diatomite from Serbia. Appl Clay Sci 43(1):33–40

Suraj G, Iyer CSP, Rugmini S, Lalithambika M (1997) The effect of micronization on kaolinites and their sorption behaviour. Appl Clay Sci 12(1–2):111–130

Suryanarayana C (2001) Mechanical alloying and milling. Prog Mater Sci 46:1–184

Wang YM, Chen TC, Yeh KJ, Shue MF (2001) Stabilization of an elevated heavy metal contaminated site. J Hazard Mater B 88:63–74

Wang S, Nan Z, Li Y, Zhao Z (2009) The chemical bonding of copper ions on kaolin from Suzhou, China. Desalination 249:991–995

White RE (1987) Introduction to the principles of soil science, 2nd edn. Blackwell, Boston